Drug oxidation by cytochrome $P450_{BM3}$: Metabolite synthesis and discovering new P450 reaction types

Xinkun Ren[a], Jake A. Yorke[a,+], Emily Taylor[a,+], Ting Zhang[b,+], Weihong Zhou*[b], and Luet Lok Wong*[a]

Abstract: There is intense interest in late-stage catalytic C–H bond functionalisation as an integral part of synthesis. Effective catalysts must have broad substrate range and tolerate diverse functional groups. Drug molecules provide a good test of these attributes of a catalyst. A library of $P450_{BM3}$ mutants developed from four base mutants with high activity for hydrocarbon oxidation produced human metabolites of a panel of drugs that included neutral (chlorzoxazone, testosterone), cationic (amitriptyline, lidocaine) and anionic (diclofenac, naproxen) compounds. No single mutant was active for all the tested drugs but multiple variants in the library showed high activity with each compound. The high conversions enabled full product characterization that led to the discovery of the new P450 reaction type of oxidative decarboxylation of a α-hydroxy carboxylic acid and the formation a protected imine from an amine, offering a novel route to α-functionalisation of amines. The substrate range and varied product profiles suggest that this library of enzymes is a good basis for developing late-stage C–H activation catalysts.

Introduction

The P450 (CYP) monooxygenases are a superfamily of *b* type cytochromes that catalyze the insertion of an oxygen atom from atmospheric dioxygen into carbon-hydrogen bonds of organic compounds. Other reaction types are known, including *N*- and *O*-dealkylation, desaturation and skeletal rearrangements.[1] Virtually all living organisms utilize P450 enzymes in the biosynthesis of steroids, vitamins and other secondary metabolites, and for the degradation and detoxification of xenobiotics. Human P450s play a vital role in drug metabolism, accounting for >90% of Phase 1 metabolic reactions.[1b] The generation of metabolites on a preparative scale is integral to drug development, as it allows for the toxicity and metabolite activity to be assessed.[2] Chemical synthesis of drug metabolites is notoriously difficult. The use of human liver microsomes is impractical due to limited availability and variable P450 levels.[3] Human P450s have been co-expressed with the cofactor protein cytochrome P450 reductase in yeast, *E. coli* and insect cells.[4] Such systems are not yet widely applicable to metabolite synthesis due to their low stability and activity.

Microbial P450s are stable, soluble and readily expressed. They offer attractive systems for the synthesis of drug metabolites and fine chemicals, and for C–H bond activation in general. $P450_{BM3}$ (CYP102A1) from *Bacillus megaterium* has been extensively investigated since it is catalytically self-sufficient and shows high activity for favored substrates.[3, 5] Rational design and high-throughput screening have increased its activity for the oxidation of numerous molecule classes, including drugs. However, even simple drug molecules such as chlorzoxazone, naproxen and lidocaine remain challenging substrates and there are few reports of product isolation and full characterization.[5b, 6] We report here a library of $P450_{BM3}$ variants which show high activity and conversion of anionic, neutral and cationic drugs to produce human drug metabolites on a preparative scale. Product characterization led to the discovery of new P450 reaction types. The crystal structure of the substrate-free form of one active mutant showed the unexpected effect of a mutation which shifted the I helix oxygen-binding groove region to the substrate-bound conformation. The more catalytically ready conformation in the mutant promotes the binding and oxidation of non-natural substrates such as drugs.

Results and Discussion

Mutant library development

The $P450_{BM3}$ mutant library was based on four variants, A330P (AP), I401P (IP), A191T/N239H/I259V/A276T/L353I (KT2) and F87A/H171L/Q307H/N319Y (KSK19) that were identified from directed evolution studies to possess increased oxidation activity for a wide range of organic compounds.[7] An initial screen of these mutants with common drugs showed detectable (by MS, data not shown) but modest activity. Inclusion of the R47L/Y51F combination (RLYF), known to promote the oxidation of non-natural substrates,[8] increased the activity (Table S1–S8). Therefore, hydrophobic substitutions of different side-chain volumes were introduced at residues (Ser72, Ala74, Val78, Phe81, Ala82, Phe87, Thr88, Ala184, Leu188, Ala328, Pro329, Ile263, Glu267) known to contact or were close to a bound substrate.[9] Six common drugs were selected as test substrates: naproxen, diclofenac, testosterone, chlorzoxazone, amitriptyline and lidocaine. Screening was conducted *in vitro* using a NADPH cofactor regeneration system. The organics were extracted and analyzed by GC and HPLC. Active mutations at two or three residues were combined; we selected residues that are not in

[a] Mr X. Ren, Dr J.A. Yorke, Miss E. Taylor, Prof. L.L. Wong*
Department of Chemistry, University of Oxford,
Inorganic Chemistry Laboratory, South Parks Road,
Oxford OX1 3QR, UK
E-mail: luet.wong@chem.ox.ac.uk
[b] Miss T. Zhang, Prof. W. Zhou*
College of Life Sciences and The State Key Laboratory of Medicinal Chemical Biology, Nankai University,
Tianjin 300071, People's Republic of China.
E-mail: zhouwh@nankai.edu.cn
[+] These authors contributed equally to the work.

Supporting information for this article is given via a link at the end of the document.

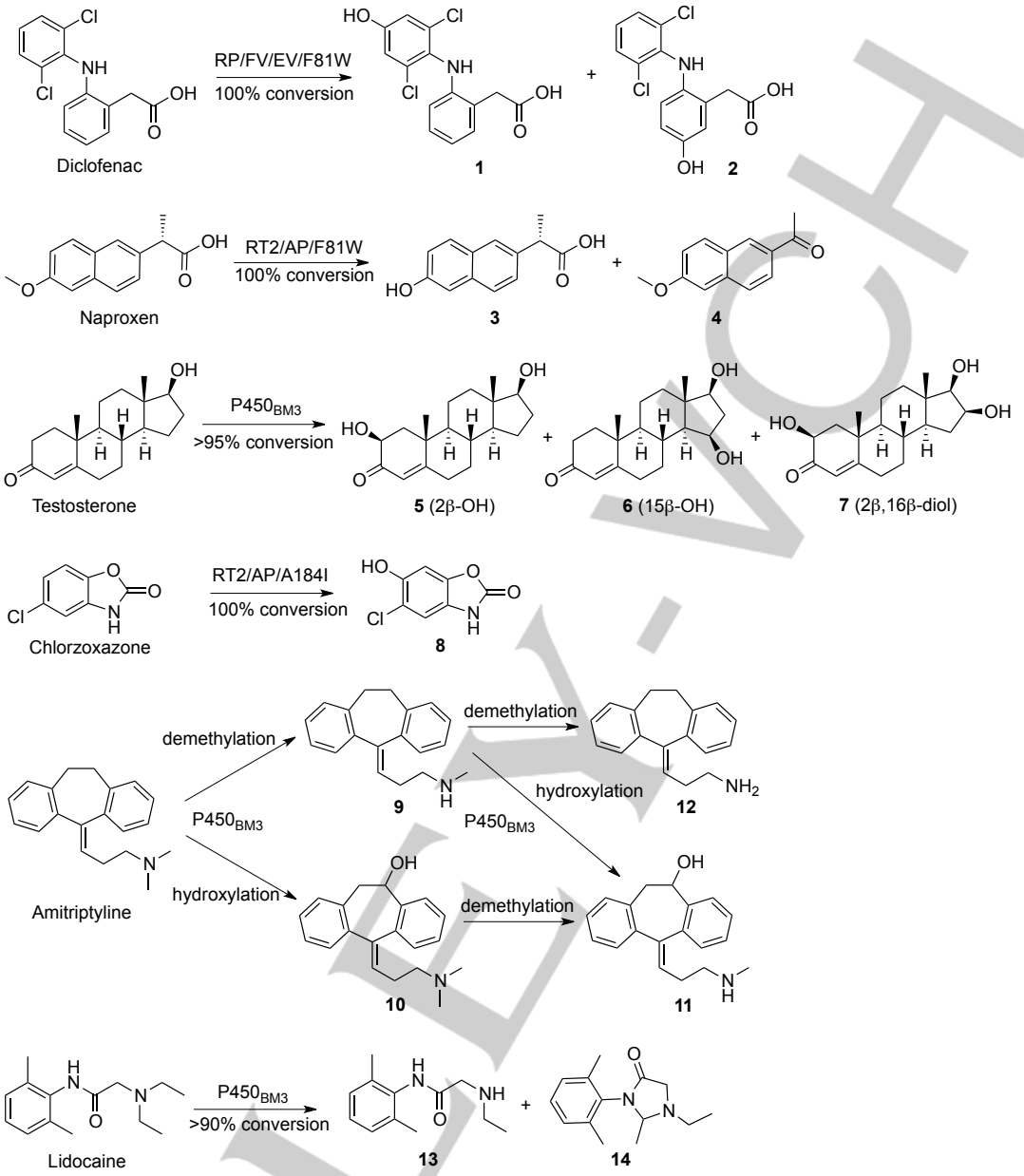

Scheme 1. Metabolism of selected drug molecules by mutants of cytochrome $P450_{BM3}$ (CYP102A1).

close proximity in order to give greater diversity in substrate pocket topology while keeping the mutant library to a manageable size (<100). After further screening, preparative scale reactions were performed for variants which gave the best conversion and highest selectivity. Products were purified by silica-gel chromatography and characterized.

Diclofenac and naproxen

Diclofenac and naproxen are common non-steroidal anti-inflammatory drugs (NSAIDs). These anionic molecules are challenging substrates for $P450_{BM3}$; variants generated by directed evolution show low activity and conversion.[6e, 10] Diclofenac is metabolized by CYP2C9 and CYP3A4 to 4'- and 5-hydroxydiclofenac. No $P450_{BM3}$ variant has been reported to have high conversion of diclofenac (the highest reported was 50%),[6d, 11] although related NSAIDs such as meclofenamic acid have been found to be oxidized.[6g] Screening of our library revealed that only mutants containing the F81W, F87V and E267V mutations showed >10% diclofenac conversion (Table S4). The RP/FV/EV mutant showed 91% conversion. Addition of the F81W mutation led to 100% conversion of 2 mM diclofenac (Table 1). The two major products were purified by silica-gel chromatography from a preparative scale reaction with the RP/FV/EV mutant and characterized as the human metabolites

4'-hydroxydiclofenac, **1** (34% yield, Fig. S9), and 5-hydroxydiclofenac, **2** (47% yield, Fig. S10) (Scheme 1). The two minor products were not formed in sufficient quantities for isolation and characterization.

Given the broad substrate range of the library the low number of hits was unexpected but consistent with the few reports of diclofenac oxidation activity by $P450_{BM3}$. Our data indicated a crucial role for a mutation at E267, with the E267V being more effective than E267F while mutations to Ile and Leu did not increase activity. It is not surprising that the F87V/E267V combination was also present in mutants that oxidized meclofenamic acid.[6g]

Table 1. Drug oxidation activity and product selectivity of some mutants of the $P450_{BM3}$ enzyme library.

Drug/variant	Conversion	Product Selectivity
Diclofenac		
RP/FV/EV	91%	**1**: 35%, **2**: 50%, **others**: 7%, 8%
RP/FV/EV/FW	100%	**1**: 45%, **2**: 55%
Naproxen		
RT2/AP/PV	96%	**3**: 66%, **4**: 34%
RT2/AP/FW	100%	**3**: 32%, **4**: 68%
RP/FV/EV	58%	**3**: 40%, **4**: 60%
Testosterone		
RLYF/KSK19	100%	**5**: 61%, **6**: 33%, **7**: 3%, **other**: 3%
RLYF/KSK19/IP	91%	**5**: 12%, **6**: 14%, **7**: 61%, **other**: 12%
KSK19	90%	**5**: – **6**: 60%, **7**: 40%
KSK19/AM	98%	**5**: 10%, **6**, 86%, **7**: 2%, **other**: 2%
KSK19/FV/QP	83%	**5**: 4%, **6**: 96%
KSK19/IA	22%	**5**: 10%, **6**: 90%
RT2/VF	89%	**5**: 5%, **6**: 95%
RP/FV/EV/AI	20%	**5**: 80%, **6**: 13%, **7**: 7%
Chlorzoxazone		
RT2/AP/AI	100%	**8**, 100%
RT2/AW/AM	97%	**8**, 100%
Amitriptyline		
KSK19	75%	**9**: 82%, **10**: 8%, **11**: 7%, **12**: 3%
RP/FV/EV	32%	**9**: 83%, **10**: 4%, **11**: 1%, **12**: 5%
RT2/AP/VI	78%	**9**: 44%, **10**: 46%, **11**: 5%, **12**: 1%
RT2/AP/AI	55%	**9**: 62%, **10**: 30%, **11**: 4%, **other**: 5%
RT2/AP/PV	21%	**9**: 64%, **10**: – **11**: 12%, **12**: 24%
Lidocaine		
RP/FV/EV	92%	**13**: 11%, **14**: 84%, **other**: 5%
RP/FV/EV/FW	93%	**13**: 96%, **14**: 4%
RT2/AW	100%	**14**: 100%

Naproxen is metabolized by CYP1A2 and CYP2C8/9/10 to the *O*-demethylation product 6-desmethylnaproxen, **3**.[12] From a screen of 44 $P450_{BM3}$ variants, 14 were found to give >40% conversion (Tables 1 & S3). Most of these contained the A330P (AP) mutation, with three RT2/AP-based variants converting >95% naproxen. The KSK19 series of mutants with the F87A mutation were also effective. The high activity of the RP/FV/EV mutant was of interest since the RP/FV and RP/EV mutants showed no conversion. All of the active mutants gave two products which were purified by silica-gel chromatography and characterized as **3** (RT2/AP/PV, 96% conversion, yield: 57%, Fig. S7) and 2-acetyl-6-methoxynaphthalene, **4** (RT2/AP/F81W, 100% conversion, yield: 62%, Fig. S8).

The novel metabolite **4** has not been reported as a product from naproxen oxidation by a P450 enzyme. It is most likely formed via α-hydroxylation followed by the new P450 reaction type of oxidative decarboxylation of a α-hydroxyacid to the ketone. We propose the mechanism shown in Scheme 2. The carboxyl radical formed by either hydrogen atom abstraction from the acid or electron transfer oxidation of the carboxylate by the ferryl, compound I species loses CO_2 and forms the ketone via abstraction of the alcohol–OH hydrogen by compound II (Fe^{IV}–OH). This mechanism is closely related to that for the decarboxylation of fatty acids with concomitant abstraction of an H-atom on the β carbon to form the terminal alkene catalyzed by the P450 enzyme $OleT_{JE}$ (CYP152L1).[13] In Scheme 2 the β H-atom is from an O–H rather than a C–H bond.

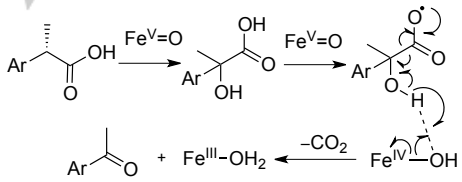

Scheme 2. Proposed mechanism for the formation of the naproxen oxidative decarboxylation metabolite 2-acetyl-6-methoxynaphthalene **4**.

α-Hydroxynaproxen, the obligatory intermediate in Scheme 2, was not observed in the reactions, indicating that it was rapidly oxidized. Indeed, α-hydroxylation of carboxylic acids is not a common P450 reaction type but is known for fatty acid oxidation by the CYP152A family of enzymes.[14] It is notable that **4** was formed by all of the mutants in our library (Table S3); even the wild type gave 20% of **4** at 5% conversion while the F87A mutant gave 48% (11% conversion). Some broad chemoselectivity trends are apparent. Bulky substitutions (A328I, A328V, A330P) favored decarboxylation while smaller side chains (P329V, I263A) promoted demethylation, e.g. the RT2/AP/F81W mutant showed 68% selectivity for naproxen decarboxylation to **4** while RT2/AP/P329V gave 66% of **3**.

Directed evolution has been applied to $P450_{BM3}$ for naproxen oxidation.[6e, 10b] Five rounds of random mutagenesis and high-throughput screening starting from the 18-mutation variant 13C9 led to the 24-mutation variant X3H1. This mutant gave 35% conversion of naproxen to a mixture of **3** and the 5,8-quinone

derivative of **3** from further oxidation. This latter product was not observed in our reactions. Since the 13C9 and X3H1 mutants also contained the F87A mutation, the other mutations probably altered naproxen binding such that **4** was not formed.[6e]

Testosterone and chlorzoxazone

Testosterone is metabolized in the human liver by CYP3A4, CYP2C9 and CYP2C19 to 1α-, 2α-/2β-, 6β-, 11β-, 15β- and 16β-hydroxytestosterone. Of the 86 variants screened, 17 showed >20% testosterone conversion (Table S5) and of these, only two (RT2/V78F and RT2/IP/A184I) did not contain a substitution of Phe87 with a smaller side chain (F87A, F87V, F87S). The RLYF/KSK19 mutant (F87A mutation) fully converted 1 mM testosterone (Fig. S3) to 61% 2β-hydroxytestosterone (**5**, Fig. S11), 33% 15β-hydroxytestosterone (**6**, Fig. S12), 3% of the new compound 2β,16β-dihydroxytestosterone (**7**, Fig. S13) and 3% of a monohydroxylated testosterone (MS data). On the other hand, the KSK19 mutant gave 60% **6** and 40% **7**. Therefore, the R47L/Y51F mutations biased the regioselectivity towards C2 oxidation to give more of **5** and disfavored further oxidation of **5** at C16 to form **7**. Addition of the I401P mutation to RLYF/KSK19 shifted the product mix further towards C2 oxidation (12% **5**, 61% **7**), with only 14% of **6** but a new product (12%) with a mass spectrum consistent with a dihydroxylated testosterone was detected. This is likely to be a further oxidation product of **6**, e.g. 2β,15β- or 15β,16β-dihydroxytestosterone. The increase in the extent of further oxidation is consistent with the previously reported effect of the I401P mutation in promoting the oxidation of a wide range of organic compounds (vide infra).[7a, 7c]

Remarkably, the KSK19/QP/FV mutant, in which the F87A mutation in KSK19 was replaced with F87V, gave 96% **6**. The RT2/V78F mutant, with V78F being the only active site mutation, gave 95% **6**. Other mutants with high selectivity for **6** included the KSK19/I263A (90%) and KSK19/A82M (86%). The V78, A82 and I263 side chains are within 6 Å of one another, suggesting that this region of the substrate pocket affects selectivity. A previous site-saturation mutagenesis study at V78 and A82 of the F87A mutant (8,700 transformants screened by HPLC) led to the V78L/A82F/F87A mutant with 91% selectivity for **6**. Starting with the mutant R47Y/T49F/F87A and screening led to the R47Y/T49F/V78L/A82M/F87A mutant which formed 96% **6**.[15]

The A82W mutation has been reported to promote testosterone 16β-hydroxylation (82%).[16] Although our mutant library did not give high selectivity for 16β-hydroxytestosterone, C16β oxidation was possible since the 2β,16β-diol **7** was formed in the reaction, e.g. KSK19 (40%) and RLYF/KSK19/IP (61%). Within our library the RP/FV/EV/A184I mutant showed the highest selectivity (80%) for C2β oxidation to give **5**, compared to the A330W/F87A mutant which gave 97%.[15] It is notable from the effects of the V78F and A82W mutations that libraries of modest size (30–100 mutants) can produce high regio- and diastereo-selectivity.

Chlorzoxazone is metabolized by CYP1A2 and CYP2E1 to 6-hydroxychlorzoxazone, **8**. Although a small 2-ring compound chlorzoxazone proved challenging even compared to the much larger testosterone. From a screen of 52 variants we found 12 with >20% chlorzoxazone conversion, of which 6 showed >50% conversion (Tables 1 & S6). In all cases **8** was the only product. The most active mutants contained bulky substitutions at A330; the RT2/A330P/A184I and RT2/A330W/A82M fully converted 1 mM chlorzoxazone (Fig. S4 and S14). A previous directed evolution study of $P450_{BM3}$ identified the mutant F162L/M185T/L188P/M237I with *ca*. 40% conversion of 200 μM chlorzoxazone to **8**.[17] None of these four mutations was in the active site. Of our library the most active mutant without a substrate pocket substitution was RT2 (51% conversion). Addition of bulky substitutions to RT2 at active site residues, especially at A330, gave 100% conversion.

Amitriptyline and lidocaine

Amitriptyline is cationic and the most commonly used tricyclic antidepressant. It is metabolized initially to nortriptyline, **9**, via demethylation and to hydroxyamitriptyline via hydroxylation, and further to *E*- and *Z*-10-hydroxynortriptyline.[18] The screen was performed with 65 variants (Table S7), of which 23 showed >20% amitriptyline conversion and the most active mutant gave 79% conversion. The base mutants RT2, KSK19 and RP had high activity, and the A330P mutation in combination with RT2 also gave high conversion (Table 1). Even the F87A single-site mutant showed 17% conversion while the RP/FV and RP/FV/EV converted 46% and 21% amitriptyline, respectively. Preparative scale reactions and product isolation showed that the human metabolite **9** was the most common product. The KSK19 mutant gave 82% **9** (Fig. S5 & S16). However, the F87A and F87V mutations strongly biased the product towards **9** while mutations added to A330P-containing variants significantly altered product selectivity. The RT2/AP/V78I mutant gave just 44% **9** but 50% *Z*-10-hydroxyamitriptyline **10**, and two other products for which the MS data were consistent with hydroxynortriptyline (**11**, 5%) and the double demethylation product desmethylnortriptyline (**12**, 1%). On the other hand, the RT2/AP/A184I gave only 30% **10** while the RT2/AP/P329V formed the highest proportions of **11** (12%) and **12** (24%) amongst the most active mutants. Interestingly, the RT2/AP/A184I/S72A mutant gave only the demethylation products **9** (25%) and **12** (75%), albeit at a low conversion of 7%, suggesting a role for the S72 side chain in binding the amine group of amitriptyline. HPLC-MS analysis in the only report of amitriptyline oxidation by $P450_{BM3}$ showed that a series of ten F87V-based mutants gave **9** as the majority product (53–71%) together with 10–15% of **12**; hydroxynortriptyline (**11**) was not formed.[6d]

Lidocaine, another cationic drug, is metabolized by CYP1A2 and CYP3A4 via de-ethylation to MEGX (**13**) and then GX, and has not been reported as a substrate for $P450_{BM3}$. From a screen of 45 variants (Table S8), 24 gave >50% lidocaine conversion. Mutants possessing enlarged (e.g. F87A and F87V) or constrained (e.g. A330P) active sites all showed high activity (Table 1). The RP/FV/EV/F81W mutant showed 93% conversion (Fig. S6) and gave 96% of the human metabolite **13** (Fig. S17). However, the RP/FV/EV mutant formed just 11% of **13** but 84% of another compound which was also the majority product for all other variants (Table S8). This compound was purified from a reaction with the RT2/A330W mutant (100% conversion, >95% yield) and characterized as the cyclic *N,N*-acetal compound (Z)-*N*-(3-ethyl-2-methyloxazolidin-5-ylidene)-2,6-dimethylaniline, **14**

(Fig. S18). This cyclization product is not a human metabolite; it was found in lidocaine metabolism by monkeys but the enzyme responsible for its formation is not known.[19]

Both **13** and **14** can be formed via spontaneous breakdown of the carbinolamine (Scheme 3), with acetaldehyde elimination competing with loss of hydroxide to form an iminium ion that is trapped by intramolecular nucleophilic attack by the amide nitrogen. If these reactions are non-enzymatic, similar product distributions should be observed for the library of $P450_{BM3}$ variants. *N*-Dealkylation is the common activity, e.g. MEGX is the primary human metabolite both *in vitro* and *in vivo*. The different behavior observed with $P450_{BM3}$ suggests different chemistry. The carbinolamine may break down within the active site, e.g. with an acidic side chain protonating the alcohol group to promote iminium ion formation in preference to acetalde hyde elimination. Alternatively, the reaction may proceed via an iminium intermediate formed by α-hydrogen atom abstraction and electron transfer oxidation. The partition between dealkylation and cyclization is determined by the competition between iminium trapping by the Fe^{III}–OH *vs*. intramolecular attack by the amide nitrogen. If the iminium carbon is far away from the Fe^{III}–OH, cyclization is more likely to occur. The product ratio depends on the effect of mutations on the mobility of the iminium group. Whatever the mechanism, the $P450_{BM3}$ mutants favor cyclization to form the *N,N*-acetal which is a protected imine and susceptible to nucleophilic attack. Since the amide nitrogen is by far the better leaving group, *N,N*-acetal formation potentially offers a novel route for α-functionalisation of amines if the enzyme can accept lidocaine-like derivatives with more complex amines in place of the diethylamino group. $P450_{BM3}$ has been shown to be a highly evolvable enzyme.[5b-d]

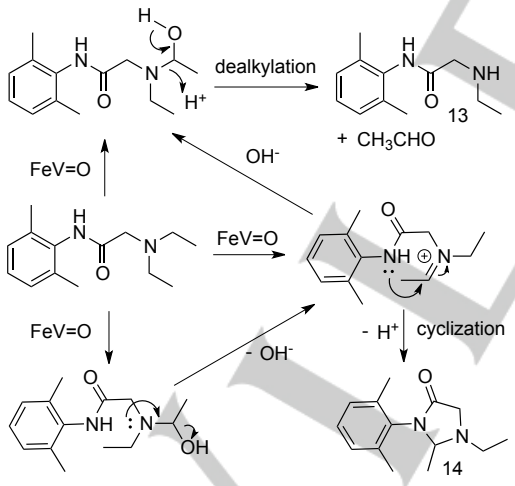

Scheme 3. Proposed mechanism for the competing pathways of de-ethylation and *N*,*N*-acetal formation in lidocaine metabolism.

Crystal structure of the RP/FV/EV mutant

The crystal structures of the substrate-free KT2, A330P and I401P mutants showed structural features that resembled the fatty acid-bound form of the wild type enzyme and promoted non-natural substrate oxidation.[7a, 7d] Of the mutations added to this base set of variants the E267V mutation had significant effects. The R47L/Y51F/F87V/E267V/I401P (RP/FV/EV) mutant was effective for the oxidation of the drugs panel. The E267V mutation removed a charged residue from the I-helix region crucial for oxygen binding and activation. The R47L/Y51F combination replaced a charged and a polar residue at the substrate channel entrance with hydrophobic ones. These two residues have been targeted in numerous $P450_{BM3}$ engineering and evolution efforts. F87 is known to play a crucial role in $P450_{BM3}$ substrate specificity and product selectivity.[5] The F87A and F87G mutations shifted lauric acid oxidation away from the ω–1 and ω–2 positions of the wild type towards the internal carbons, giving as much as 34% ω–5 oxidation.[20] The F87I mutation, on the other hand, gave 57% ω–1 and 5% of ω, terminal oxidation of palmitic acid.[21] The crystal structure of the substrate-free form of the RP/FV/EV mutant was determined to provide further insight into $P450_{BM3}$ activity and specificity.

Arg47 and Tyr51 are located on one strand of the β1 sheet.[9] The Y51F mutation did not cause any conformation changes but the R47L led to tilting of the β-strand to bury the hydrophobic Leu side chain in the protein interior (Fig. 1A). As a result the channel entrance is narrower and less polar than in the wild type (Fig. S19), which will alter the substrate specificity. The structure around V87 is unchanged compared to the wild type, and space is created in the vicinity of the heme by this mutation, consistent with the expanded substrate range of the mutant.

The I401P mutation, adjacent to the heme proximal residue Cys400, has been shown to cause the proximal loop and the heme to drop away from the substrate pocket to adopt the substrate-bound conformation.[7a] This key structural feature was preserved in the RP/FV/EV mutant (Fig. 1B). In the I401P mutant these movements lengthened the Fe–OH_2 distance to 3.6 Å. This weakened axial water interaction led to the heme reduction potential (–302 mV) and the rate constant (254 s^{-1}) of the first electron transfer step for substrate-free I401P being comparable those (–317 mV and 226 s^{-1}) for the palmitic acid-bound wild type.[7a] As a result the requirement for a non-natural substrate to induce the displacement of the axial water to initiate the catalytic cycle is much reduced, and the I401P mutation promotes non-natural substrate oxidation by $P450_{BM3}$.

Glu267 forms a salt bridge with Lys440 in both the substrate-free and fatty acid-bound wild type structures. Conformational changes in the E435–K440 β-turn on fatty acid binding is accompanied by movement of the K440 and E267 side chains. This salt bridge is broken in the mutant, and the K440 side-chain NH_2 forms a H-bond with the T436 side-chain OH (Fig. 1B). Without a salt bridge to K440 the V267 side chain moved towards the substrate binding pocket and may play a role in substrate binding in the mutant. The E435–K440 β-turn in the mutant closely resembles that in the substrate-bound wild type structure (Fig. 1B). The I helix and in particular the oxygen-binding groove between A264 and T268 become superimposable onto that of the substrate-bound wild type structure. This conformational change in the wild type structure is driven by fatty acid binding and its adaptation in the substrate-

free form lowers the barrier to non-natural substrate binding. This structural feature was observed for the KT2 mutant [7d] but not the I401P.[7a] On the other hand, the KT2 mutant does not possess the proximal loop movement of the I401P. The combination of these two structural features indicates that the substrate-free form of the RP/FV/EV mutant is in a catalytically ready conformation and can show enhanced oxidation activity for non-natural substrates compared to the RP, RT2 and RP/FV variants. Similar hydrophobic substitutions will cleave the E267-K440 salt bridge and likely lead to similar oxygen-binding groove conformation changes to promote non-natural substrate oxidation while altered side chain volume could affect substrate binding and product selectivity.

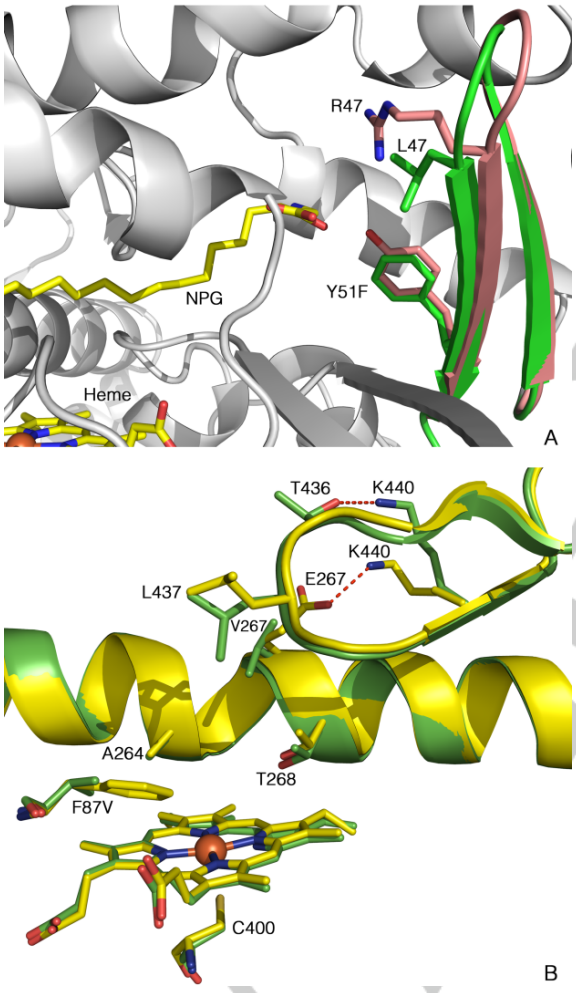

Figure 1. (A) Distortion of the β strand at the substrate channel entrance of substrate-free R47L/Y51F/I401P/F87V/E267V (RP/FV/EV, green, PDB code: 4RSN) as a result of the R47L mutation compared with the substrate-free wild type (salmon, PDB code: 1BU7) and with *N*-palmitoylglycine (NPG, yellow) in the NPG-bound wild type structure (PDB code: 1JPZ) included for comparison. (B) The key elements of the active site structure of substrate-free RP/FV/EV (green) and NPG-bound WT $P450_{BM3}$ (yellow) showing the substrate-bound position of the heme and Cys400, the new H-bond between Lys440 and Thr436, the substrate-bound conformations of the I helix and β turn around L437, and movement of a V267 γ-methyl towards the substrate pocket.

Conclusions

The library of $P450_{BM3}$ variants oxidized the panel of cationic, anionic and neutral drug compounds to human metabolites and revealed a new P450 reaction type. No single mutant or family of mutants showed high conversion with all the tested drugs but the mutant library gave full coverage and with varied product profiles. The formation of a stable, protected imine via cyclization of lidocaine offers a novel route for α-functionalisation of amines. There is intense interest in late-stage C–H bond functionalisation as a means to streamline synthesis. A pre-requisite for this is an enzyme collection with wide substrate range, excellent functional group tolerance, diverse product selectivity and high conversion to maximize the likelihood of initial hits for further selectivity optimization. The results suggest that the library of $P450_{BM3}$ variants is the basis for one such collection.

Experimental Section

General

General reagents, buffers and chemicals were from Alfa-Aesar, ThermoFisher Scientific and Sigma-Aldrich, UK. Enzymes for molecular biology were from New England Biolabs, UK. All the drug compounds were from Sigma-Aldrich except for chlorzoxazone which was from Alfa-Aesar. Geduran Silica Gel 60, 40–63 μm from ThermoFisher Scientific was used for column chromatography. DNA and microbiological manipulations were carried out by standard methods. Site-directed mutagenesis was carried out by a PCR-based method using the KOD Hot Start Polymerase kit from Merck Biosciences, UK. Oligonucleotides were from Eurofins MWG Biotech, Germany.
The $P450_{BM3}$ enzymes were produced in *Escherichia coli* BL21 (DE3) and purified by anion exchange chromatography, as previously described.[7a] The enzymes were stored as 10 μM stocks in 1-mL aliquots at –20 ºC and thawed on ice before use.

Drug oxidation

Oxidation of drugs by $P450_{BM3}$ mutants was screened in 0.5 mL assays using a NADPH regeneration system, 1–2 μM P450, 50 mM Tris-HCl (pH 8.5) or 200 mM phosphate buffer (pH 7.5). Substrate (0.5–2 mM) was added from a 50 mM ethanol stock (testosterone) or a 100 mM ethanol stock (all other drugs). Glucose dehydrogenase (Codexis, USA) was added (2 U/mL) along with glucose (100 mM). $NADP^+$ monosodium salt was added to a final concentration of 80 μM and the reaction mixtures were shaken at 200 rpm for 16 h at 25 ºC. The aqueous phase was extracted with 300 μL of ethyl acetate (or diethyl ether for cationic compounds) and analysed by GC or HPLC. Full details on the mutant panel and screening results are provided in the Supplementary Material.

Oxidation of diclofenac

The 50 mL reaction mixture in 200 mM phosphate buffer, pH 7.5, contained 5 μM of the RP/FV/EV/F81W variant, 2 mM diclofenac sodium salt (31.8 mg, 2 mM added as a 100 mM ethanol stock), 2 U/mL glucose dehydrogenase and 100 mM glucose. $NADP^+$ monosodium salt was added to a final concentration of 80 μM (4 mM stock in 200 mM phosphate buffer, pH 7.5) to initiate the reaction. After stirring at 500 rpm at room temperature for 2 hours the reaction mixture was extracted with

EtOAc (50 mL × 3). Control experiments showed that acidifying the mixture before extraction did not give more product. The combined EtOAc extracts were dried over $MgSO_4$ and the solvent was removed after filtration. The residue was subjected to silica-gel column chromatography, eluting with dichloromethane and then petroleum ether/Et_2O to give 11 mg (34%) of 4'-hydroxydiclofenac, **1,** and 14.6 mg (47%) of 5-hydroxydiclofenac, **2**, after removal of solvent. **4′-Hydroxydiclofenac, 1:** ^{1}H NMR (500 MHz, CD_3OD) δ 7.91 (s, 1H), 7.18 (dd, *J* = 7.5, 1.4 Hz, 1H), 7.04 (td, *J* = 7.8, 1.5 Hz, 1H), 6.89 (s, 2H), 6.82 (td, *J* = 7.4, 1.1 Hz, 1H), 6.27 (dd, *J* = 8.1, 1.1 Hz, 1H), 3.72 (s, 2H). ^{13}C NMR (126 MHz, CD_3OD) δ 176.32, 156.59, 145.77, 133.91, 132.11, 130.78, 129.12, 124.62, 121.57, 117.17, 116.68, 39.65. HRMS (APCI) [M+Na$^+$] Calcd for $C_{14}H_{11}Cl_2NO_3$: 334.0008, Found: 334.0013. **5-Hydroxydiclofenac, 2:** ^{1}H NMR (500 MHz, CD_3OD) δ 7.34 (d, *J* = 8.1 Hz, 1H), 6.96 (t, *J* = 8.1 Hz, 1H), 6.70 (d, *J* = 2.8 Hz, 1H), 6.54 (dd, *J* = 8.6, 2.8 Hz, 1H), 6.36 (d, *J* = 8.6 Hz, 1H), 3.70 (s, 1H). ^{13}C NMR (126 MHz, CD_3OD) δ 176.20, 154.39, 140.84, 136.63, 130.32, 129.69, 129.44, 122.12, 118.59, 115.49, 39.58. HRMS (APCI) [M+Na$^+$] Calcd for $C_{14}H_{11}Cl_2NO_3$: 334.0008, Found: 334.0013.

Oxidation of naproxen

The 50 mL reaction mixture in 200 mM phosphate buffer, pH 7.5, contained 2 μM of the RT2/AP/PV variant, 100 mM glucose, 2 U/mL glucose dehydrogenase and naproxen sodium salt (1 mM, 12.6 mg, from a 100 mM methanol stock). NADP$^+$ monosodium salt was added to a final concentration of 80 μM (4 mM stock in 200 mM phosphate buffer, pH 7.5) to initiate the reaction. After stirring at 500 rpm at room temperature for 2 hours the reaction mixture was extracted with EtOAc (50 mL × 3). The combined EtOAc extracts were dried over $MgSO_4$ and the solvent was removed after filtration. The residue was subjected to silica-gel column chromatography, eluting with petroleum ether and then petroleum ether/Et_2O to give 6.2 mg (57%) of 6-desmethylnaproxen, **3**, after removal of solvent. **6-Desmethylnaproxen**, **3**: ^{1}H NMR (500 MHz, CD_3OD) δ = 7.69 – 7.57 (m, 3H), 7.35 (dd, *J* = 8.5, 1.9 Hz, 1H), 7.09 – 7.01 (m, 2H), 3.81 (q, *J* = 7.1 Hz, 1H), 1.51 (d, *J* = 7.3 Hz, 3H). ^{13}C NMR (126 MHz, CD_3OD) δ = 177.18, 155.01, 135.40, 134.09, 128.89, 128.45, 126.13, 125.67, 125.53, 118.10, 108.34, 45.16, 17.63. HRMS (APCI) [M+Na$^+$] Calcd for $C_{12}H_{18}N_2O$: 239.0683, Found: 239.0679.

2-Acetyl-6-methoxynaphthalene, **4**, was generated and isolated (11.6 mg, 62%) from a 100 mL reaction with 2 μM of the RT2/AP/F81W variant by the same method as for **3**. **2-Acetyl-6-methoxynaphthalene**, **4**: ^{1}H NMR (500 MHz, $CDCl_3$) δ = 8.41 (d, *J* = 2.0 Hz, 1H), 8.02 (dd, *J* = 8.7, 1.9 Hz, 1H), 7.87 (d, *J* = 8.8 Hz, 1H), 7.78 (d, *J* = 8.7 Hz, 1H), 7.22 (dd, *J* = 9.0, 2.5 Hz, 1H), 7.17 (d, *J* = 2.5 Hz, 1H), 3.96 (s, 3H), 2.71 (s, 3H). ^{13}C NMR (126 MHz, $CDCl_3$) δ = 198.09, 159.96, 137.48, 132.82, 131.32, 128.01, 127.29, 124.87, 119.93, 105.94, 55.63, 26.76. HRMS (APCI) [M+Na$^+$] Calcd for $C_{13}H_{12}O_3$: 233.0730, Found: 233.0731.

Oxidation of testosterone

The 50 mL reaction mixture in 200 mM phosphate buffer, pH 7.5, contained 1 μM of the RLYF/KSK19 variant, testosterone (14.4 mg, 1 mM added from a 100 mM methanol stock), 2 U/mL glucose dehydrogenase and 100 mM glucose. NADP$^+$ monosodium salt was added to a final concentration of 80 μM (4 mM stock in 200 mM phosphate buffer, pH 7.5) to initiate the reaction. After stirring at 500 rpm at room temperature for 2 hours the reaction mixture was extracted with EtOAc (50 mL × 3). The combined EtOAc extracts were dried over Na_2SO_4 and the solvent was removed after filtration. The residue was subjected to silica-gel column chromatography eluting with petroleum ether/EtOAc to give 8.4 mg (55%) of **2β-hydroxytestosterone**, **5**. ^{1}H NMR (500 MHz, $CDCl_3$) δ = 5.81 (d, *J* = 1.2 Hz, 1H), 4.19 (dd, *J* = 13.9, 5.6 Hz, 1H), 3.67 (t, *J* = 8.6 Hz, 1H), 3.51 – 3.46 (m, 1H), 2.57 – 2.46 (m, 2H), 2.29 – 2.23 (m, 1H), 2.18 (s, 3H), 2.08 (tdd, *J* = 9.3, 7.6, 4.2 Hz, 1H), 2.02 – 1.95 (m, 1H), 1.92 – 1.86 (m, 1H), 1.80 (ddd, *J* = 13.4, 7.0, 3.8 Hz, 1H), 1.71 (ddd, *J* = 13.9, 10.7, 4.1 Hz, 1H), 1.64 – 1.37 (m, 9H), 1.36 – 1.25 (m, 2H), 1.19 (s, 3H), 1.14 (td, *J* = 12.8, 4.1 Hz, 1H), 1.06 – 0.96 (m, 2H), 0.80 (s, 3H). ^{13}C NMR (126 MHz, CDCl3) δ = 199.90, 175.28, 118.86, 81.66, 68.72, 50.67, 50.39, 43.58, 41.64, 39.64, 36.56, 36.05, 34.74, 33.18, 30.65, 23.53, 23.02, 22.73, 11.42. HRMS (APCI) [M+H$^+$] Calcd for $C_{19}H_{28}O_3$: 305.2111, Found: 305.2111.

The oxidation of testosterone to generate 15β-hydroxytestosterone, **6,** was performed following the same procedure as for **5** but utilizing 1 μM of the RT2/V78F variant. 11.8 mg of **6** was isolated after silica-gel column chromatography using a petroleum ether/EtOAc solvent system. **15β-Hydroxytestosterone**, **6**: ^{1}H NMR (500 MHz, $CDCl_3$) δ = 5.75 (s, 1H), 4.23 (ddd, *J* = 7.8, 5.7, 2.4 Hz, 1H), 3.59 (t, *J* = 8.7 Hz, 1H), 2.64 (ddd, *J* = 14.6, 8.6, 7.7 Hz, 1H), 2.53 – 2.28 (m, 4H), 2.18 (s, 1H), 2.14 – 1.95 (m, 3H), 1.85 (dt, *J* = 12.3, 3.2 Hz, 1H), 1.72 (td, *J* = 14.0, 4.7 Hz, 1H), 1.66 – 1.51 (m, 9H), 1.46 (ddd, *J* = 13.0, 6.5, 3.9 Hz, 2H), 1.24 (d, *J* = 5.8 Hz, 3H), 1.18 – 0.96 (m, 7H). ^{13}C NMR (126 MHz, CDCl3) δ = 199.70, 171.12, 124.16, 81.31, 69.33, 55.36, 54.47, 43.63, 42.43, 38.97, 38.06, 35.98, 34.16, 32.86, 31.67, 31.24, 20.76, 17.52, 13.90. HRMS (APCI) [M+H$^+$] Calcd for $C_{19}H_{28}O_3$: 305.2111, Found: 305.2111.

The oxidation of testosterone to generate 2β,16β-dihydroxytestosterone, **7**, was performed following the same protocol as for **5** but utilizing 1 μM of the RLYF/KSK19/IP variant. 7.6 mg of 2β,16β-hydroxytestosterone, **7**, was isolated after silica-gel column chromatography using a petroleum ether/EtOAc solvent system. **2β,16β-Dihydroxytestosterone**, **7:** ^{1}H NMR (500 MHz, $CDCl_3$) δ = 5.83 (d, *J* = 1.0 Hz, 1H), 4.19 (dd, *J* = 13.1, 5.0 Hz, 1H), 3.60 (t, *J* = 8.7 Hz, 1H), 3.52 – 3.44 (m, 1H), 2.69 – 2.56 (m, 2H), 2.50 (dd, *J* = 13.8, 5.6 Hz, 1H), 2.30 (dt, *J* = 7.1, 6.0 Hz, 2H), 2.18 (s, 3H), 1.95 – 1.77 (m, 2H), 1.68 – 1.31 (m, 6H), 1.32 – 1.19 (m, 2H), 1.19 – 1.04 (m, 4H). ^{13}C NMR (126 MHz, $CDCl_3$) δ = 199.69, 174.97, 118.71, 81.02, 69.23, 68.54, 55.16, 50.69, 43.62, 42.83, 41.62, 39.53, 37.89, 33.99, 32.95, 32.01, 22.84, 22.51, 13.92. HRMS (APCI) [M+H$^+$] Calcd for $C_{19}H_{29}O_4$: 321.2060, Found: 321.2062.

Oxidation of chlorzoxazone

The 50 mL reaction mixture in 200 mM phosphate buffer, pH 7.5, contained 2 μM of the RT2/AP/A184I variant, chlorzoxazone (17.0 mg, 2 mM added from a 100 mM ethanol stock), 2 U/mL glucose dehydrogenase and 100 mM glucose. NADP$^+$ monosodium salt was added to a final concentration of 80 μM from a 4 mM stock in 200 mM phosphate buffer (pH 7.5), to initiate the reaction. The reaction mixture was stirred at 500 rpm at room temperature for 2 hours and then extracted with EtOAc (50 mL × 3). The combined EtOAc extracts were dried over $MgSO_4$ and the solvent was removed after filtration. The residue was subjected to silica-gel column chromatography eluting with petroleum ether and then petroleum ether/Et_2O to give 18.1 mg (98%) of 6-hydroxychlorzoxazone, **8**, after removal of solvent. **6-Hydroxychlorzoxazone, 8**: ^{1}H NMR (500 MHz, CD_3OD) δ = 6.94 (s, 1H), 6.75 (s, 1H). ^{13}C NMR (126 MHz, CD_3OD) δ = 155.92, 148.86, 143.29, 123.25, 115.57, 110.21, 98.82. HRMS (APCI) [M+Na$^+$] Calcd for $C_7H_4ClNO_3$: 207.9772, Found: 207.9767.

Oxidation of amitriptyline

The 50 mL reaction mixture in 50 mM Tris-HCl, pH 8.5, contained 2 μM of the KSK19 variant, amitriptyline hydrochloride monohydrate (31.3 mg, 2 mM, added as a 100 mM ethanol stock), 2 U/mL glucose dehydrogenase and 100 mM glucose. NADP$^+$ monosodium salt was added to a final concentration of 80 μM (4 mM stock in 50 mM Tris-HCl, pH 8.5) to initiate the reaction. The reaction mixture was stirred at 500 rpm under O_2 at room temperature for 2 hours, adjusted to pH>12 with 5 M KOH and extracted with Et_2O (50 mL × 3). The combined Et_2O

extracts were dried over $MgSO_4$ and the solvent was removed after filtration. The residue was subjected to silica-gel column chromatography, eluting with $CHCl_3$ and then $CHCl_3$/MeOH/NH_4OH (90:10:0.1) to give 9.78 mg (69%) of **nortriptyline**, **9**: ^{1}H NMR (400 MHz, $CDCl_3$) δ 7.34 – 7.28 (m, 1H), 7.24 – 7.11 (m, 6H), 7.08 – 7.03 (m, 1H), 5.87 (t, *J* = 7.4 Hz, 1H), 3.48 – 3.25 (m, 2H), 3.08 – 2.90 (m, 1H), 2.79 (d, *J* = 8.4 Hz, 1H), 2.67 (t, *J* = 6.9 Hz, 2H), 2.40 (s, 3H), 2.34 (dt, *J* = 14.3, 7.2 Hz, 4H). ^{13}C NMR (101 MHz, $CDCl_3$) δ = 144.32, 141.38, 140.13, 139.42, 137.22, 130.15, 129.36, 128.73, 128.49, 128.20, 127.59, 127.25, 126.18, 125.94, 51.94, 36.40, 33.94, 32.24, 30.03. HRMS (APCI) [M+Na$^+$] Calcd for C19H21N: 286.1566, Found: 286.1568.

The 100 mL scale oxidation of amitriptyline to generate (*Z*)-10-hydroxyamitriptyline, **10**, was performed following the protocol for **9** using 2 μM of the RT2/AP/V78I variant and 61.6 mg of amitriptyline hydrochloride monohydrate. 18.7 mg of **10** was isolated after silica-gel column chromatography, eluting with $CHCl_3$ and then $CHCl_3$/MeOH/NH_4OH (90:10:0.1). **10** was identified by comparison with published NMR data.[22] HRMS (APCI) [M+H$^+$] Calcd for $C_{20}H_{23}NO$: 294.1848, Found: 294.1852.

Oxidation of lidocaine

The 25 mL reaction mixture in 50 mM Tris-HCl, pH 8.5, contained 1 μM of the RP/FV/EV/F81W variant, 14.44 mg lidocaine hydrochloride monohydrate (2 mM, added from a 100 mM ethanol stock), 2 U/mL glucose dehydrogenase and 100 mM glucose. NADP$^+$ monosodium salt was added to a final concentration of 80 μM (4 mM stock in 50 mM Tris-HCl, pH 8.5) to initiate the reaction. The reaction mixture was stirred at 500 rpm at room temperature for 2 hours and then adjusted to pH>12 with 5 M KOH and extracted with Et_2O (25 mL × 3). The combined Et_2O extracts were dried over $MgSO_4$ and the solvent was removed after filtration. The residue was subjected to silica-gel column chromatography eluting with $CHCl_3$ and then $CHCl_3$/MeOH/NH_4OH (90:10:0.1) to give 8.8 mg (85%) of **MEGX**, **13**. ^{1}H NMR (500 MHz, $CDCl_3$) δ = 8.84 (br s, 1H), 7.16 – 7.05 (m, 3H), 3.47 (s, 2H), 2.80 (q, *J* = 7.1 Hz, 2H), 2.24 (s, 2H), 1.61 (br s, 1H), 1.19 (t, *J* = 7.1 Hz, 1H). ^{13}C NMR (126 MHz, $CDCl_3$) δ = 170.36 (C(O)NH), 135.25, 134.02, 128.39, 127.25, 52.75, 45.03, 18.73, 15.69. HRMS (APCI) [M+Na$^+$] Calcd for $C_{12}H_{18}N_2O$: 229.1311, Found: 229.1314.

The 25 mL scale oxidation of lidocaine to generate the *N,N*-acetal **14** was performed following the method for **13** except for utilizing 1 μM of the RT2/A330W variant and the reaction mixture was stirred under O_2 at room temperature for 2 hours. After extraction with Et_2O (25 mL × 3), the combined Et_2O extracts were dried over $MgSO_4$ and the solvent was removed after filtration. The residue was subjected to silica-gel column chromatography, eluting with petroleum ether/Et_2O (50:50 then 0:100) to give 11.6 mg (95%) of **(*Z*)-*N*-(3-ethyl-2-methyloxazolidin-5-ylidene)-2,6-dimethylaniline**, **14**. ^{1}H NMR (500 MHz, $CDCl_3$) δ = 7.20 – 7.05 (m, 3H), 4.50 – 4.45 (m, 1H), 3.79 (dd, *J* = 14.7 Hz, 1.2, 1H), 3.19 (dd, *J* = 14.7, 1.7 Hz, 1H), 3.00 – 2.89 (m, 1H), 2.54 – 2.43 (m, 1H), 2.28 (s, 3H), 2.22 (s, 3H), 1.19 (t, *J* = 7.2 Hz, 3H), 1.15 (d, *J* = 5.7 Hz, 3H). ^{13}C NMR (126 MHz, $CDCl_3$) δ = 170.37, 138.16, 135.94, 133.23, 128.99, 128.83, 128.58, 77.36, 55.37, 47.70, 18.96, 18.84, 18.47, 13.56. HRMS (APCI) [M+Na$^+$] Calcd for $C_{12}H_{18}N_2O$: 255.1468, Found: 255.1477.

Crystallisation and structure determination

The sitting-drop vapor-diffusion method was used with Crystal Screen kits I & II and Index (Hampton Research) to grow crystals of the heme domain of the RP/FV/EV mutant at 16 °C in 48-well plates. Two drops (each of 1 μL) of the protein solution at 30 or 50 mg mL^{-1} protein were mixed with 1 μL reservoir solution and equilibrated against 100 μL reservoir solution. Dark red crystals can be seen from condition No.1 of Screen Kit II, and condition No. 85 of Index screen kits after one week. Crystal optimisation was performed with the hanging-drop vapor-diffusion method by varying the buffer pH, the concentration of precipitant, the protein concentration, and volume ratio of protein to reservoir solution. Good diffraction-quality crystals could be obtained in 3–4 days by using similar conditions to No. 1 of the Index kit, e.g. 2.0 M sodium chloride, 10% w/v PEG 6000. Crystals were flash-frozen before data collection; no cryoprotectant was used. X-ray diffraction data were collected at the Shanghai Synchrotron Radiation Facility (SSRF) beamline BL17U. The crystals belonged to space group P31, with unit-cell parameters *a* = *b* = 78.30 Å, *c* = 203.19 Å, and two molecules in each asymmetric unit. The structure was solved by the molecular-replacement method using Phaser in the CCP4 suite and the structure of the A330P mutant (PDB: 3M4V) as a search model.[7a] The initial model was rebuilt with Coot [23] and refined with REFMAC5 and Phenix.refine.[24] The stereochemical quality of the refined structure was checked with the program MolProbity.[25] A summary of the data collection and structure refinement statistics is provided in Table S9. The coordinates of the crystal structure have been deposited in the PDB with accession code: 4RSN.

Acknowledgments

We thank Professor Jeremy Robertson and Mr Jack O'Hanlon for helpful discussion. Xinkun Ren is supported by the China Oxford Scholarship Fund and Jake A. Yorke by NSERC, Canada, and The Rhodes Trust.

Keywords: cytochrome P450 • C–H activation • decarboxylation • drug metabolism • protein engineering

[1] a) P. R. Ortiz de Montellano, 'Cytochrome P450: Structure, Mechanism, and Biochemistry' 3rd ed., Kluwer Academic/Plenum Press, New York, **2005**; b) F. P. Guengerich, *Chem. Res. Toxicol.* **2007**, *21*, 70-83; c) P. R. Ortiz de Montellano, *Chem. Rev.* **2009**, *110*, 932-948; dF. P. Guengerich, A. W. Munro, *J. Biol. Chem.* **2013**, *288*, 17065-17073.

[2] F. P. Guengerich, *Chem. Res. Toxicol.* **2009**, *22*, 237-238.

[3] V. B. Urlacher, M. Girhard, *Trends Biotechnol.* **2012**, *30*, 26-36.

[4] a) T. H. Rushmore, P. J. Reider, D. Slaughter, C. Assang, M. Shou, *Metab. Eng.* **2000**, *2*, 115-125; b) R. B. Vail, M. J. Homann, I. Hanna, A. Zaks, *J. Ind. Microbiol. Biotechnol.* **2005**, *32*, 67-74; c) I. Neunzig, A. Goehring, C.-A. Dragan, J. Zapp, F. T. Peters, H. H. Maurer, M. Bureik, *J. Biotechnol.* **2012**, *157*, 417-420.

[5] a) R. Bernhardt, *J. Biotechnol.* **2006**, *124*, 128-145; b) C. J. Whitehouse, S. G. Bell, L. L. Wong, *Chem. Soc. Rev.* **2012**, *41*, 1218-1260; c) S. T. Jung, R. Lauchli, F. H. Arnold, *Curr. Opin. Biotechnol.* **2011**, *22*, 809-817; d) G. D. Roiban, M. T. Reetz, *Chem. Commun.* **2015**, *51*, 2208-2224.

[6] a) B. M. van Vugt-Lussenburg, E. Stjernschantz, J. Lastdrager, C. Oostenbrink, N. P. Vermeulen, J. N. Commandeur, *J. Med. Chem.* **2007**, *50*, 455-461; b) M. C. Damsten, B. M. van Vugt-Lussenburg, T. Zeldenthuis, J. S. de Vlieger, J. N. Commandeur, N. P. Vermeulen, *Chem. Biol. Interact.* **2008**, *171*, 96-107; c) A. M. Sawayama, M. M. Chen, P. Kulanthaivel, M. S. Kuo, H. Hemmerle, F. H. Arnold, *Chem. Eur. J.* **2009**, *15*, 11723-11729; d) J. Reinen, J. S. van Leeuwen, Y. Li, L. Sun, P. D. Grootenhuis, C. J. Decker, J. Saunders, N. P. Vermeulen, J. N. Commandeur, *Drug Metab. Disposit.* **2011**, *39*, 1568-1576; e) A. Rentmeister, T. R. Brown, C. D. Snow, M. N. Carbone, F. H. Arnold, *ChemCatChem* **2011**, *3*, 1065-1071; f) G. Di Nardo, G. Gilardi, *Int. J. Mol. Sci.* **2012**, *13*, 15901-15924; g) H. Venkataraman, M. C. Verkade-Vreeker, L. Capoferri, D. P. Geerke, N. P. Vermeulen, J. N. Commandeur, *Bioorg. Med. Chem.* **2014**, *22*, 5613-5620.

[7] a) C. J. Whitehouse, W. Yang, J. A. Yorke, B. C. Rowlatt, A. J. Strong, C. F. Blanford, S. G. Bell, M. Bartlam, L. L. Wong, Z. Rao, *ChemBioChem* **2010**, *11*, 2549-2556; b) C. J. C. Whitehouse, S. G. Bell, H. G. Tufton, R. J. P. Kenny, L. C. I. Ogilvie, L.-L. Wong, *Chem. Commun.* **2008**, 966-968; c) C. J. C. Whitehouse, S. G. Bell, W. Yang, J. A. Yorke, C. F. Blanford, A. J. F. Strong, E. J. Morse, M. Bartlam, Z. Rao, L.-L. Wong, *ChemBioChem* **2009**, *10*, 1654-1656; d) C. J. Whitehouse, W. Yang, J. A. Yorke, H. G. Tufton, L. C. Ogilvie, S. G. Bell, W. Zhou, M. Bartlam, Z. Rao, L. L. Wong, *Dalton Trans.* **2011**, *40*,

10383-10396; e) R. J. P. Kenny, Part II thesis, University of Oxford **2005**.
[8] A. B. Carmichael, L. L. Wong, *FEBS J.* **2001**, *268*, 3117-3125.
[9] H. Li, T. L. Poulos, *Nat. Struct. Biol.* **1997**, *4*, 140-146.
[10] a) M. Landwehr, L. Hochrein, C. R. Otey, A. Kasrayan, J. E. Backvall, F. H. Arnold, *J. Am. Chem. Soc.* **2006**, *128*, 6058-6059; b) J. D. Bloom, S. T. Labthavikul, C. R. Otey, F. H. Arnold, *Proc. Natl. Acad. Sci. U S A* **2006**, *103*, 5869-5874.
[11] G. E. Tsotsou, A. Sideri, A. Goyal, G. Di Nardo, G. Gilardi, *Chem. Eur. J.* **2012**, *18*, 3582-3588.
[12] A. D. Rodrigues, M. J. Kukulka, E. M. Roberts, D. Ouellet, T. R. Rodgers, *Drug Metab. Dispos.* **1996**, *24*, 126-136.
[13] a) M. A. Rude, T. S. Baron, S. Brubaker, M. Alibhai, S. B. Del Cardayre, A. Schirmer, *Appl. Environ. Microbiol.* **2011**, *77*, 1718-1727; b) J. Belcher, K. J. McLean, S. Matthews, L. S. Woodward, K. Fisher, S. E. Rigby, D. R. Nelson, D. Potts, M. T. Baynham, D. A. Parker, D. Leys, A. W. Munro, *J. Biol. Chem.* **2014**, *289*, 6535-6550.
[14] D. S. Lee, A. Yamada, H. Sugimoto, I. Matsunaga, H. Ogura, K. Ichihara, S. I. Adachi, S. Y. Park, Y. Shiro, *J. Biol. Chem.* **2003**, *278*, 9761-9767.
[15] S. Kille, F. E. Zilly, J. P. Acevedo, M. T. Reetz, *Nat. Chem.* **2011**, *3*, 738-743.
[16] V. Rea, A. J. Kolkman, E. Vottero, E. J. Stronks, K. A. Ampt, M. Honing, N. P. Vermeulen, S. S. Wijmenga, J. N. Commandeur, *Biochemistry* **2012**, *51*, 750-760.
[17] S. H. Park, D. H. Kim, D. Kim, D. H. Kim, H. C. Jung, J. G. Pan, T. Ahn, D. Kim, C. H. Yun, *Drug Metab. Dispos.* **2010**, *38*, 732-739.
[18] a) O. V. Olesen, K. Linnet, *Pharmacology* **1997**, *55*, 235-243; b) O. V. Olesen, K. Linnet, *Drug Metab. Dispos.* **1997**, *25*, 740-744.
[19] G. D. Breck, W. F. Trager, *Science* **1971**, *173*, 544-546.
[20] M. Dietrich, T. A. Do, R. D. Schmid, J. Pleiss, V. B. Urlacher, *J. Biotechnol.* **2009**, *139*, 115-117.
[21] F. Brühlmann, L. Fourage, C. Ullmann, O. P. Haefliger, N. Jeckelmann, C. Dubois, D. Wahler, *J. Biotechnol.* **2014**, *184*, 17-26.
[22] N. Lassen, J. Perregaard, *Acta Chem. Scand.* **1983**, *37*, 335-340.
[23] P. Emsley, K. Cowtan, *Acta Crystallogr. D: Biol. Crystallogr.* **2004**, *60*, 2126-2132.
[24] a) G. N. Murshudov, P. Skubak, A. A. Lebedev, N. S. Pannu, R. A. Steiner, R. A. Nicholls, M. D. Winn, F. Long, A. A. Vagin, *Acta Crystallogr. D Biol. Crystallogr.* **2011**, *67*, 355-367; b) P. V. Afonine, R. W. Grosse-Kunstleve, N. Echols, J. J. Headd, N. W. Moriarty, M. Mustyakimov, T. C. Terwilliger, A. Urzhumtsev, P. H. Zwart, P. D. Adams, *Acta Crystallogr. D Biol. Crystallogr.* **2012**, *68*, 352-367.
[25] V. B. Chen, W. B. Arendall, 3rd, J. J. Headd, D. A. Keedy, R. M. Immormino, G. J. Kapral, L. W. Murray, J. S. Richardson, D. C. Richardson, *Acta Crystallogr. D: Biol. Crystallogr.* **2010**, *66*, 12-21.

Entry for the Table of Contents

FULL PAPER

The scalable oxidation of a panel of drug molecules by a library of $P450_{BM3}$ mutants generated human metabolites on a preparative scale and led to the discovery of new P450 reaction types, indicating that the library may be a good source of late-stage C–H activation catalysts.

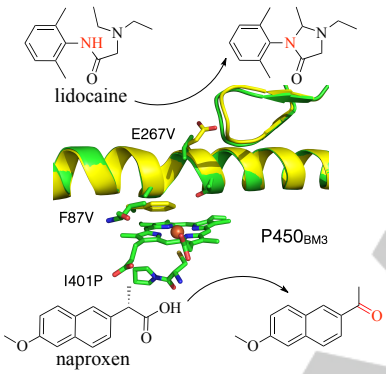

Xinkun Ren, Jake A. Yorke, Emily Taylor, Ting Zhang, Weihong Zhou, Luet Lok Wong**

Page No. – Page No.

Drug oxidation by cytochrome $P450_{BM3}$: Metabolite synthesis and discovering new P450 reaction types